Kinetic Inductance Detectors (KIDs) for the SAFARI Instrument on SPICA

L. Ferrari[*a], A. M. Baryshev[a,b], J. J. A. Baselmans[a], G. de Lange[a], P. Diener[a], J. W. Kooi[c], J.J. Lankwarden[a], S. J. C. Yates[a]

[a]SRON National Institute for Space Research, Sorbonnelaan 2, Utrecht, The Netherlands;
[b]Kapteyn Astronomical Institute, University of Groningen, Landleven 12, Groningen, The Netherlands;
[c]California Institute of Technology, MS 320-47, Pasadena, Ca 91125, USA

ABSTRACT

Kinetic Inductance Detectors (KIDs) with frequency domain read-out are intrinsically very suitable to use as building blocks for very large arrays. KIDs therefore are an attractive detector option for the SAFARI instrument on SPICA, Millimetron and also for large scale ground based imaging arrays. To study the properties of large KID arrays we have fabricated 400 pixels array made from 40 nm thick Al films on high resistivity Si substrates. The array is tested in a dry dilution refrigerator at 100 mK. We present the device design and experimental results. We also present a new design of the array with lithographic air bridges over the coplanar waveguide feedline. The air bridges are designed to suppress the slot line mode in the feedline and that will improve the pixel to pixel reproducibility of large arrays.

Keywords: Kinetic Inductance Detectors, frequency spacing, air-bridges.

1. INTRODUCTION

SPICA (Space Infrared telescope for Cosmology and Astrophysics) [1]is an astronomical mission optimized for mid and far-infrared astronomy with a cryogenically cooled 3 m telescope, able to extend our investigation beyond the James Webb Space Telescope. Its high spatial resolution and unprecedented sensitivity in the mid and far infrared will address strategic problems of the present-day astronomy like star formation history of the Universe or planets formation. SPICA is proposed as a Japanese-led mission with an extensive international collaboration. The far-infrared instrument has been studied mostly by European Consortium and the instrument is named SAFARI (SPICA Far-Infrared Instrument).

The baseline optical configuration of SAFARI is an imaging Fourier Transform Spectrometer (FTS). Principal advantages of this type of spectrometer are:

- High mapping speed due to the spectral multiplexing.
- Ability to incorporate a photometric imaging mode.
- Operational flexibility to tailor the spectral resolution to the science programs.

The properties of the spectrometer (as scanning speed of the moving mirrors and required frequency resolution) set the speed of the detectors with a minimum response of 20 Hz. Quicker detectors would enable quicker scans and would be considered an advantage. For a Nyquist sampled diffraction limited observation, the load and hence the photon noise per pixel is constant, and given by the source and bandwidth of observation. For SPICA it is about $3 \cdot 10^{-19}$ W/Hz$^{0.5}$ NEP; as a consequence the goal for every pixel is NEP $2 \cdot 10^{-19}$ W/Hz$^{0.5}$. The instrument should cover as much as possible of the telescope field of view. The baseline specification gives 6000 pixels split into 3 bands of octave bandwidth (see Table 1). The requirements of 6000 pixels is 3 times larger than is actually done in space, while $2 \cdot 10^{-19}$ W/Hz$^{0.5}$ is an order of magnitude lower than currently optically demonstrated, even in current

[*] lorenza@sron.nl; phone +31 (0)50 363 8321; fax +31 (0)50 363 4033; www.sron.nl

Space Telescopes and Instrumentation 2010: Optical, Infrared, and Millimeter Wave, edited by Jacobus M. Oschmann Jr., Mark C. Clampin, Howard A. MacEwen, Proc. of SPIE Vol. 7731, 77314H · © 2010 SPIE · CCC code: 0277-786X/10/$18 · doi: 10.1117/12.868529

laboratory experiments. In order to meet the challenging requirements a study of different detector technologies was considered by the Consortium. In the current design stage the possible detector options are: Transition Edge Sensors (TESs), photoconductors, Si bolometers and KIDs [2].

A very important and useful feature of the KIDs, technology that we are investigating, is the possibility to multiplex the read-out using frequency division multiplexing very easily. A Q factor of 10^6 would enable in principle to read-out more than 10.000 resonators in one GHz bandwidth. For this purpose the study of the frequency spacing of the pixels is necessary and the pixel to pixel reproducibility is crucial. We have fabricated and characterized a 20x20 array for the 35-60 μm of SAFARI and the results are shown on the following sections.

Table 1. SAFARI bands, giving center wavelength, pixel size for different optical configurations, pixel size (D = 3.5 mm) on sky and number pixels/band. For an optical configuration of f/20, considered the instrument baseline, the array size is 32x32 mm for all 3 bands.

Band (μm)	λ_c (μm)	Fλ/2 (μm)			1.22λ/D (arcsec)	Number of pixels
		f/10	f/20	f/40		
35-60	48	240	480	960	3.6	64x64
60-110	85	420	850	1680	6.1	38x38
110-210	160	800	1600	3200	11.5	20x20

2. KINETIC INDUCTANCE DETECTORS

In a superconducting material electrons around the Fermi energy are paired into bosonic particles called Cooper pairs consisting each of 2 electrons with opposite spin that condensate into one macroscopic quantum state [3]. At nonzero temperature some thermally excited single particles remain, called quasiparticles, which behave in most ways as normal electrons. In the 2-fluid model a superconductor is described as a parallel circuit with a (kinetic) inductance due to the condensate and a resistive part due to any remaining quasiparticles. Hence the complex surface conductivity at non-zero frequencies reacts to an AC signal.

In a MKID, quasiparticles created by incident radiation are sensed by measuring the change in the surface impedance of a superconductor film $Z_s = R_s + i\omega L_s$ where R_s is the resistive term associated with the quasiparticles, and L_s the kinetic inductance due to the Cooper pairs. This change is read-out by making the superconducting film part of a resonant circuit (see Figure 1), capacitively coupled to a through line with the result that it will form a short circuit at resonance. The absorption of a photon causes the resonance center frequency to shift to lower values (due to the increase of L_s, reduction in Cooper pairs) and to make the measured dip in the transmission smaller (due the increase of R_s, quasiparticles number increase). Both effects together produce a phase change at the original resonance frequency f_0. This phase change as a function of quasiparticles number is the signal we read-out to measure the absorption of a photon.

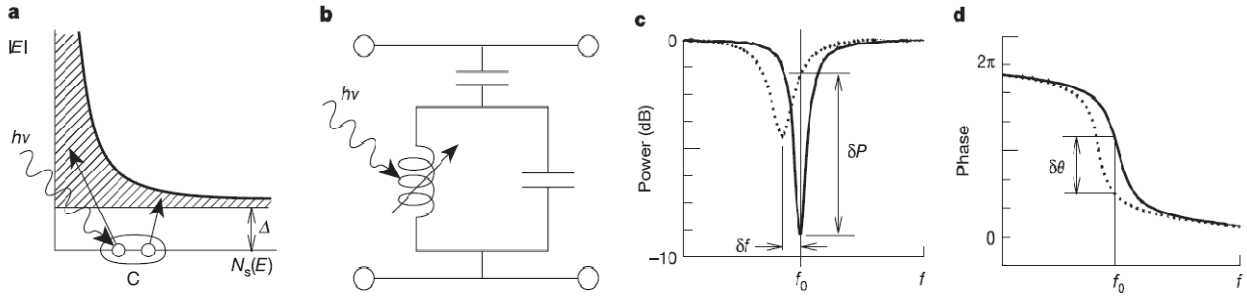

Figure 1. Panel a) photon with energy $h\nu > 2\Delta$ (Δ is the superconducting gap energy) is absorbed in a superconducting film and breaks Cooper pairs and creates a number of quasiparticles excitations. Panel b shoes the resonant circuit, depicted as a parallel LC circuit which is capacitively coupled to a through line. Panel c shows that on resonance, the

LC circuit loads the through line, producing a dip in its transmission. The quasiparticles produced by the photon increase both L_s and R_s, which moves the resonance to lower frequency and makes the dip shallower. Both effects contribute to changing the amplitude (panel c) and phase (panel d) of a microwave probe signal transmitted past the circuit. Picture taken from [4]

3. DESIGN

For the study of the pixels frequency spacing, we have designed an array made only with resonator without antenna or absorber. The resonator consists of a superconducting coplanar waveguide (CPW) with a length of $\frac{1}{4}\lambda$, where λ is the wavelength corresponding to the resonance frequency. In the $\frac{1}{4}\lambda$ resonator the central conductor is shorted at the far end to the ground plane and floating at the coupler end, where it is coupled capacitively to the through line by letting it run parallel with it (see Figure 2). The length of the coupler and the distance between the through line and the part of the resonator running parallel with it determines the coupling Q of the resonator Q_c. The key for the operation of the MKID is the fact that the Q factor of the superconductor is determined by the ratio of the imaginary and real part of the complex surface inductance, which increases exponentially with decreasing the temperature.

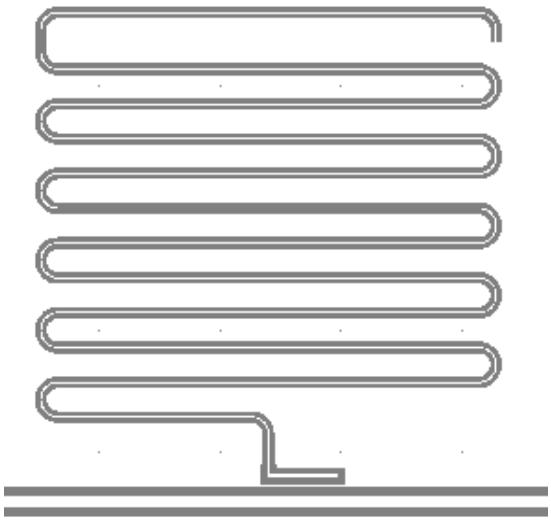

Figure 2 A quarter-wavelength resonator, capacitively coupled to a feed-line, formed by the superconducting film.

The array is 20 x 20 pixels with a designed Q of 600.000. The spacing between 2 pixels is 0.48 mm. The designed frequency spacing of the pixels is 1 MHz. The chosen superconductor material is Al that it has a low critical temperature TC and a long quasiparticles lifetime. The film of Al is 40 nm thick sputtered on high-resistivity Silicon substrate.

4. TEST

Testing KIDs requires cooling devices to temperature around 10% of their superconducting transition temperature. For aluminum resonator, the working temperature is about 100 mK. The tests were performed in a dry dilution refrigerator from Leiden Cryogenics in SRON Groningen. The read-out signal is brought inside the cryostat with coaxial cables. Four Copper-Nickel coaxial cables bring the signal from room temperature at the top of the cryostat to the 50K plate. The input signal goes through a cold 30 dB attenuator and DC block. After the 50 K plate niobium-titanium coax are used to bring the signal to the cold stage because of them low thermal conductivity. Immediately and after the resonator are 80 GHz low pass filters. The resonators reside in a sample box inside a cryoperm magnetic shield. The sample box is designed to be light tight. In the output channel the signal is amplified by a low-noise 4-8 GHz HEMT cold amplifier from Yebes. The readout channel is completed by other 2 warm Miteq commercial amplifiers.

We measured the fraction of the transmitted power, denoted by S21, as a function of frequency using an IQ-mixer (see Figure 3). A microwave frequency synthesizer creates a signal which is split in two by a microwave signal splitter. One copy goes into the LO port of an IQ mixer. The other copy goes through the cryostat, resonators and amplifiers back to the RF port of the IQ mixer. Ideally this detection scheme, called homodyne mixing because the same signal is used for the LO and RF, produces as an output value the real part of the transmission signal in the I channel and the imaginary part in the Q channel. In reality, the I and Q values we get from a real IQ mixer need to be scaled to account for the conversion losses of the channels and other imperfections (like phase balance and leakage) in order to get the calibrated data of the transmission. The use of the IQ mixer permits also the measurement of the noise and lifetime of the quasiparticles.

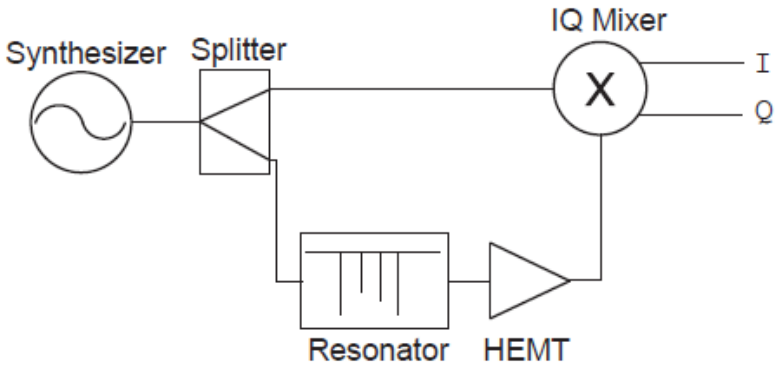

Figure 3 the circuit diagram of a homodyne detection scheme.

5. RESULTS

We measured the S21 transmission as function of frequency at 100 mK. We made a power sweep in order to find the value of power on the KIDs level giving an high response without overdriven the resonators. The measurements are performed with a microwave power of -98 dBm at the resonator (see Figure 4). We found all 400 pixels as we expected in a frequency range between 5.2 and 5.6 GHz.

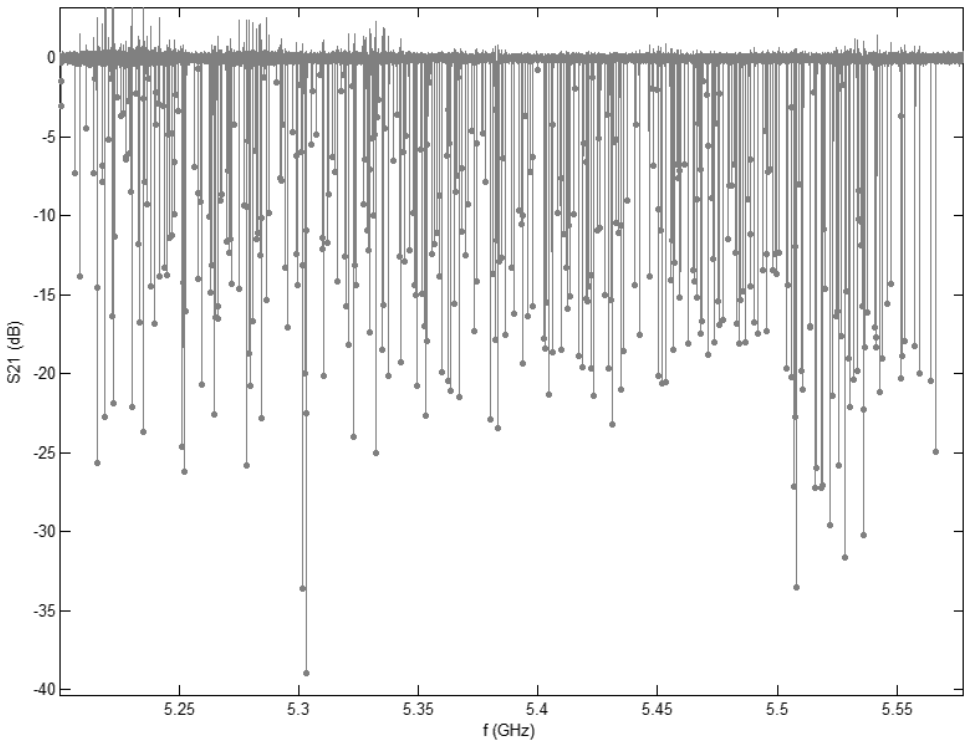

Figure 4: S21 transmission as function of frequency. Measured at 100 mK with a power of -98 dBm on the resonator level.

From the resonance dip bandwidth we can calculate the Q factor resonator using:

$$Q = \frac{f_0}{2\delta f} \tag{1}$$

where the bandwidth 2δ corresponds to the frequency difference between the 2 points in the resonance curve where S_{21} is given by:

$$|S_{21}|^2 = \frac{\left|S_{21}^{min}\right|^2 + 1}{2} \tag{2}$$

with S_{21}^{min} the transmission of the KID at the resonance frequency. For an infinitely deep KID $\left|S_{21}^{min}\right|^2 = 0$ and $\left|S_{21}^{min}\right|^2 = 1/2$ corresponding to a -3dB width measured down from the carrier amplitude. The measured Q can be expressed as a combination from the coupling Q_c and the factor associated with any other losses Q_i:

$$\frac{1}{Q} = \frac{Q_c + Q_i}{Q_c Q_i} \tag{3}$$

using the measured resonance feature and:

$$Q_i = \frac{Q}{S_{21}^{min}} \tag{4}$$

We can obtain Q_c, Q and Q_i. Note that Q_c should be identical to the design Q factor. Q_i is associated with losses in the resonator. This includes quasiparticles losses due to nonzero temperatures, radiation losses from the CPW; dielectric losses; losses in the film, including quasiparticles at high temperature or optical loading. In Figure 5 is shown the distribution of the Q, Q_c and Q_i and we can observe the mean value of the Q factor is 600.000 a value comparable to the designed one, but there is a large scatter on the Q factor and dip depth. The frequency spacing between pixels is 0.90 MHz with a 0.7 MHz scatter Gaussian like, value in agreement with the design one. That it is a good result, indicating that we are able to multiplex a thousand of pixels in 1 GHz bandwidth avoiding pixels loss.

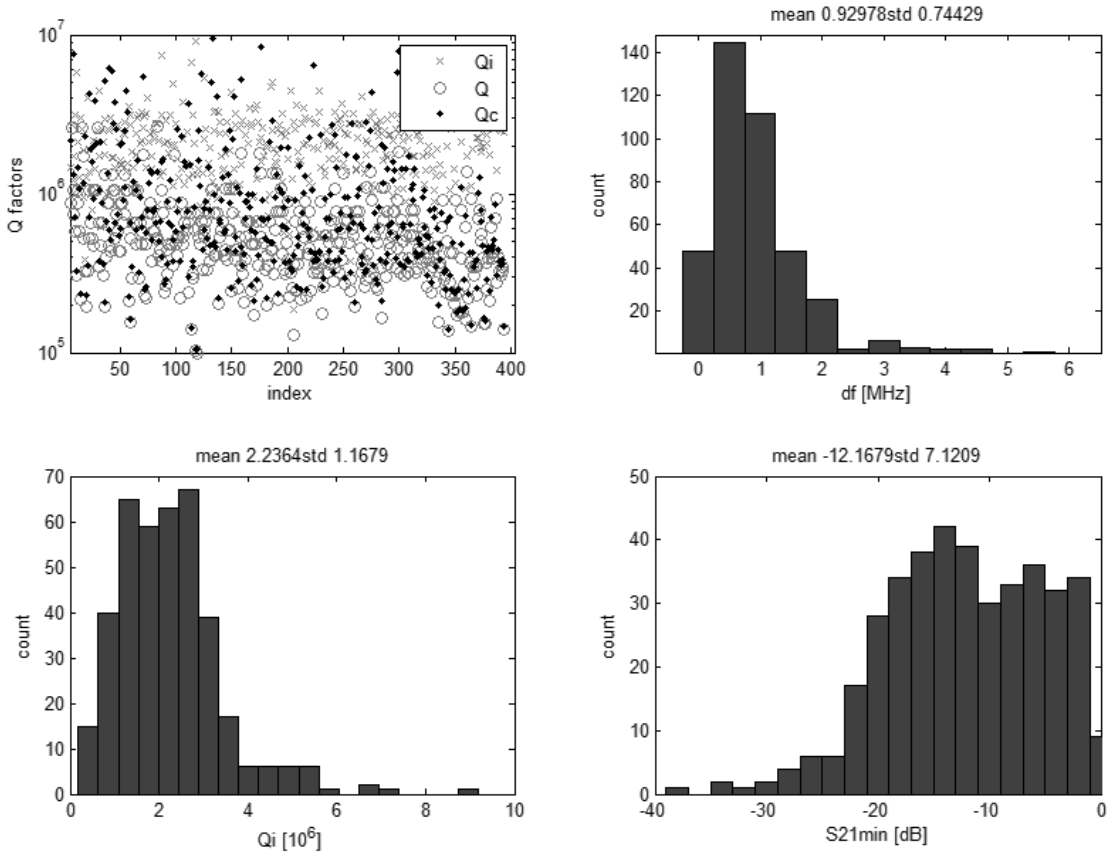

Figure 5 In the left top panel is reported the internal coupling Q_i, Q_c and the total Q factor distribution in function of the resonators. In the right top panel the distribution of the frequency spacing is plotted. In the left bottom panel is reported the distribution of the internal coupling Q_i factor. In the right bottom panel the dip depth distribution is plotted.

We repeated the measurements at different temperatures which showed the same behavior.

6. SIMULATION

In order to investigate the problem of Q scatter and improve the reproducibility of the frequency spacing we are performing a simulation using HFSS [5]. We have observed in the past that the presence of wire bonds in between the KIDs reduces the variation in Q factors. In the simulation the effect of air-bridges is studied and the optimum position on the array is also investigating. The use of lithographic air-bridges instead of wire bonds is obviously preferable because of reliability and reproducibility on the fabrication process.

In Figure 6 it is reported the model simulated in HFSS: it consists in a CPW feed line with 3 identical elbow couplers with 1 port each with and without 24 μm air-bridges around the couplers.

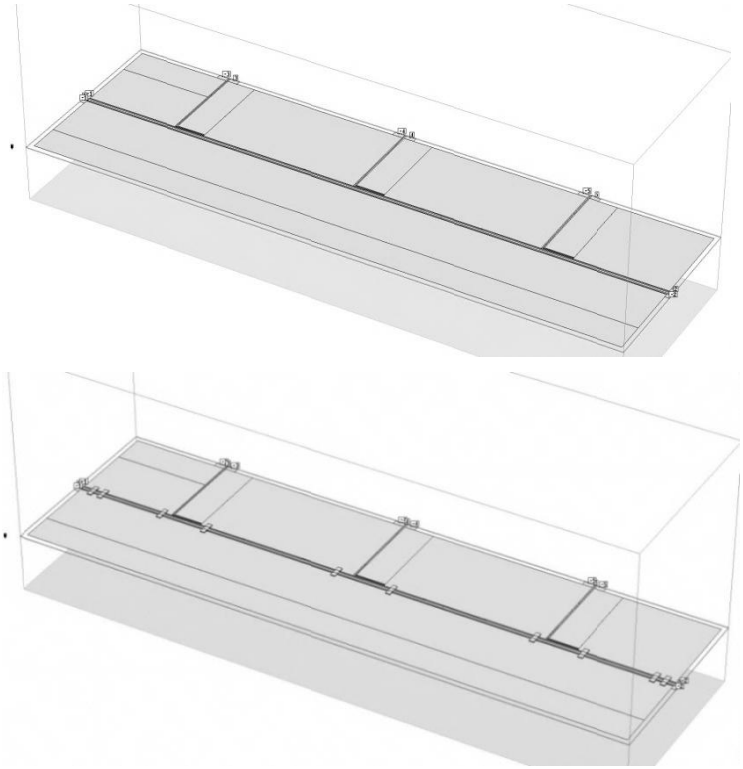

Figure 6: The model simulated of the CPW feedline with 3 identical elbow couplers without (on the top) and with air-bridges around all couplers (on the bottom).

We excited the three ports and plotted the electric field in the even and odd mode (see Figure 7 and Figure 8). Any odd modes generated in the KID can mutual couple with other resonators. The presence of air-bridges on the feedline suppresses the odd mode and cleans up the scatter in the even mode. This will reduce the scatter on the factor due to reduction of undesired coupling between the resonators.

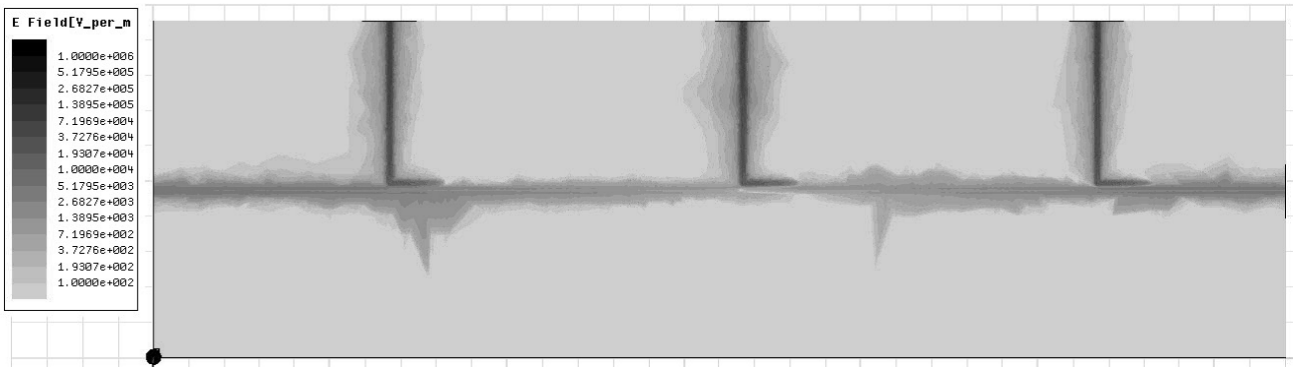

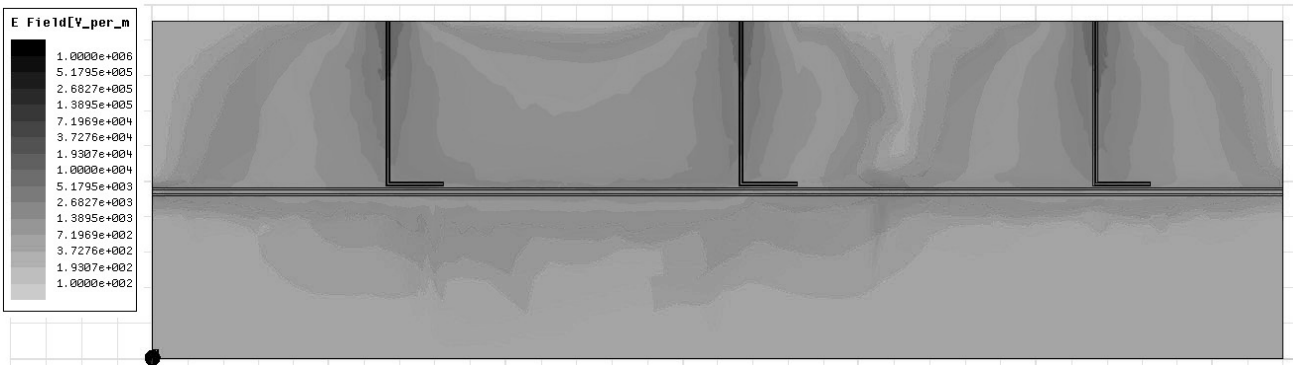

Figure 7: E-field on Si substrate, 3 ports excited and no air bridges. On the top the even mode is reported and the odd mode is on the bottom graph.

Figure 8: E-field on Si substrate, 3 ports excited with 24 m air bridges. On the top the even mode is reported and the odd mode is on the bottom graph.

The fabrication of large array with lithographic air-bridges is now under investigation, the process requires a tuning on the fabrication procedure in order to have robust bridges and reproducibility on the quality of fabrication.

7. CONCLUSION

We have designed and fabricated a large high array of 20 x 20 pixels for the 35-60 μm band of SAFARI. The chip has been tested in a dry dilution fridge at 100 mK. The results show a good agreement between the theoretical and experimental properties, in particular the frequency spacing between resonators. We have also observed much scatter on the Q factor distribution than we expected. To solve this problem we are performing a simulation using HFSS. The model predicts that the use of air-bridges over the feedline suppresses the odd mode reducing the

coupling between resonators and as a consequence the Q scatters. The fabrication of large array with 24 μm is now under process.

ACKNOWLEDGEMENT

The technical assistance of W. J. Vreeling, W. Horinga and L. de Jong is gratefully acknowledged.

REFERENCES

[1] Swinyard, B.M., "The SAFARI far infrared imaging Fourier transform spectrometer for the SPICA Mission," Proc. SPIE 7731-26, (2010)
[2] Day, P.K., Leduc, H.G., Mazin, B.A., Vayonakis A., Zmuidzinas J., "A superconducting detector suitable for use in large arrays," Nature, 425, 817–821, (2003).
[3] Tinkham M., [Introduction to Superconductivity]. McGraw–Hill, New York, second ed.,(1996).
[4] Mazin, B., Ph.D. Thesis, Caltech, (2004)
[5] HFSS website: http://www.ansoft.com/products/hf/hfss/.